RESEARCH ARTICLE

Dendritic Cell-Specific Antigen Delivery by Coronavirus Vaccine Vectors Induces Long-Lasting Protective Antiviral and Antitumor Immunity

Luisa Cervantes-Barragan,[a,b] Roland Züst,[a] Reinhard Maier,[a] Sophie Sierro,[c] Jozef Janda,[c] Frederic Levy,[c] Daniel Speiser,[c] Pedro Romero,[c] Pierre-Simon Rohrlich,[d,e,f] Burkhard Ludewig,[a,g] and Volker Thiel[a,g]

Institute of Immunobiology, Kantonal Hospital St. Gallen, St. Gallen, Switzerland[a]; Unidad de Investigación Médica en Inmunoquímica, Hospital de Especialidades, Centro Médico Nacional Siglo XXI, IMSS, México City, México[b]; Ludwig Institute for Cancer Research, Lausanne, Switzerland[c]; INSERM U645-IFR133, Besançon, France[d]; University of Besançon, Besançon, France[e]; CHU Besançon, Service de Pédiatrie, Besançon, France[f]; and VetSuisse Faculty, University of Zurich, Zurich, Switzerland[g]

V.T. and B.L. share senior authorship.

ABSTRACT **Efficient vaccination against infectious agents and tumors depends on specific antigen targeting to dendritic cells (DCs). We report here that biosafe coronavirus-based vaccine vectors facilitate delivery of multiple antigens and immunostimulatory cytokines to professional antigen-presenting cells *in vitro* and *in vivo*. Vaccine vectors based on heavily attenuated murine coronavirus genomes were generated to express epitopes from the lymphocytic choriomeningitis virus glycoprotein, or human Melan-A, in combination with the immunostimulatory cytokine granulocyte-macrophage colony-stimulating factor (GM-CSF). These vectors selectively targeted DCs *in vitro* and *in vivo* resulting in vector-mediated antigen expression and efficient maturation of DCs. Single application of only low vector doses elicited strong and long-lasting cytotoxic T-cell responses, providing protective antiviral and antitumor immunity. Furthermore, human DCs transduced with Melan-A-recombinant human coronavirus 229E efficiently activated tumor-specific CD8$^+$ T cells. Taken together, this novel vaccine platform is well suited to deliver antigens and immunostimulatory cytokines to DCs and to initiate and maintain protective immunity.**

IMPORTANCE **Vaccination against infectious agents has protected many individuals from severe disease. In addition, prophylactic and, most likely, also therapeutic vaccination against tumors will save millions from metastatic disease. This study describes a novel vaccine approach that facilitates delivery of viral or tumor antigens to dendritic cells *in vivo*. Concomitant immunostimulation via the cytokine granulocyte-macrophage colony-stimulating factor (GM-CSF) was achieved through delivery by the same viral vector. Single immunization with only low doses of coronavirus-based vaccine vectors was sufficient to elicit (i) vigorous expansion and optimal differentiation of CD8$^+$ T cells, (ii) protective and long-lasting antiviral immunity, and (iii) prophylactic and therapeutic tumor immunity. Moreover, highly efficient antigen delivery to human DCs with recombinant human coronavirus 229E and specific stimulation of human CD8$^+$ T cells revealed that this approach is exceptionally well suited for translation into human vaccine studies.**

Received 22 June 2010 **Accepted** 16 August 2010 **Published** 14 September 2010

Citation Cervantes-Barragan, L., R. Züst, R. Maier, S. Sierro, J. Janda, et al. 2010. Dendritic cell-specific antigen delivery by coronavirus vaccine vectors induces long-lasting protective antiviral and antitumor immunity. mBio 1(4):e00171-10. doi:10.1128/mBio.00171-10.

Editor Peter Palese, Mount Sinai School of Medicine

Address correspondence to Burkhard Ludewig, burkhard.ludewig@kssg.ch, and Volker Thiel, volker.thiel@kssg.ch.

Vaccination against viral infections has saved millions of lives by protecting many individuals from diseases such as measles, rubella, mumps, and polio. However, there is a growing need not only to develop improved vaccines against such acute infections but also to generate therapeutic vaccines which can stimulate specific immune responses to persistent viruses such as the human immunodeficiency virus or the human hepatitis C virus (1, 2). Likewise, novel approaches for vaccination against tumors which counteract the immunosuppression associated with cancer are needed (3). There is compelling evidence that CD8$^+$ cytotoxic T cells are crucial players in the protective immune response against viral infections and tumors (4). Novel vaccine approaches should thus be rigorously evaluated for their ability to maximally expand antigen-specific CD8$^+$ T cells, to induce their optimal differentiation into effector CD8$^+$ T cells, and to elicit long-lasting protective memory (4).

A major bottleneck in the development of new and effective vaccines is the delivery of antigens to dendritic cells (DCs) (5, 6), which sample the antigen, transport immunogenic components to secondary lymphoid organs, and initiate and maintain T and B cell responses. The excellent capacity of DCs to prime protective antiviral T cell responses has been shown *in vivo* (7–9). Likewise, several preclinical studies demonstrated that efficient antitumor immunity can be induced using adoptive transfer of DCs (10–12). Although individualized adoptive transfer of antigen-loaded DCs is feasible and, to a certain extent, efficient in clinical applications to humans (13), off-the-shelf vaccines that permit targeted delivery of antigens to DCs *in vivo* have become a major focus in vaccine development. Consequently, the description of cell surface molecules that, for example, exhibit a rather specific expression by DCs has fueled the development of antibody-based targeting

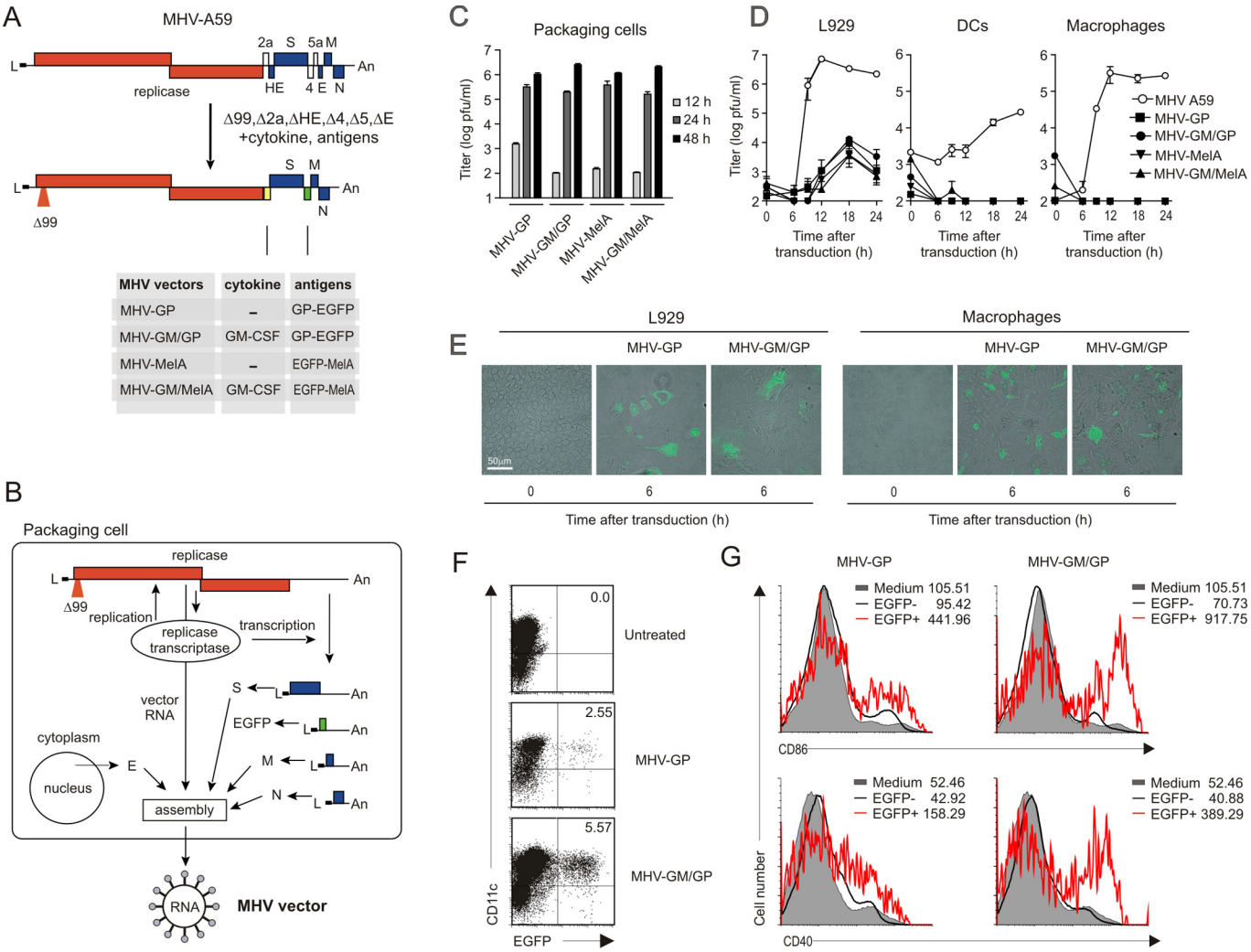

FIG 1 Generation, propagation, and *in vitro* target cell tropism of MHV-based vaccine vectors. (A) Schematic representation of the MHV-A59 genome and the highly attenuated MHV vectors. (B) Packaging concept for the generation of replication-competent but propagation-deficient MHV particles. (C) Growth kinetics of the indicated MHV vectors in 17ECl20 packaging cells. Cells were infected at an MOI of 1, and titers in supernatants were determined at the indicated time points (means of results from triplicate measurements ± standard errors of the means [SEM]). (D) Replication of the indicated MHV vectors or MHV-A59 wild-type virus in L929 cells, bone marrow-derived DCs, and peritoneal macrophages. The indicated cells (10^6/ml, MOI = 1) were infected, and replication was monitored by titration of supernatants on 17ECl20 packaging cells (mean ± SEM of duplicate measurements). One representative experiment out of three is displayed. (E) Transduction of L929 cells and peritoneal macrophages with an MHV-GP or MHV-GM/GP vector (MOI = 1). Green fluorescence was recorded 6 h posttransduction. Original magnification, ×400. (F, G) Stimulation of DCs by GM-CSF-expressing vectors. Bone marrow-derived DCs (10^6) from B6 mice were transduced with the indicated MHV-based vector (MOI = 1) or left untreated. Cells were harvested 12 h later and stained for CD11c, CD86, and CD40 expression. (F) Representative dot plots indicating the high transduction efficacy. Values in the upper right quadrant indicate percentages of $EGFP^+$ cells. (G) Expression of the DC activation markers CD86 and CD40 on untreated $CD11c^+$ cells (shaded), on $CD11c^+$ $EGFP^+$ cells (thick black line), or on $CD11c^+EGFP^-$ cells (thick red line). Values in the histograms represent mean fluorescence intensity of the respective population.

strategies (14–16). These protein-based vaccines generate $CD4^+$ T cell and B cell responses against a range of different antigens. However, antigen coupling to antibodies is a major limitation for the induction of $CD8^+$ T cell responses which are strictly dependent on cross-presentation (5, 17). In contrast, viral vectors encoding immunogenic antigens can deliver their genetic cargo directly into DCs, thus generating antigenic peptides in infected cells and allowing for efficient loading of major histocompatibility complex (MHC) class I molecules. Among the currently most exploited virus systems that facilitate antigen delivery to DCs are adenoviral (18, 19), lentiviral (20), arenaviral (21), and alphaviral (22, 23) systems. However, major impediments of these vectors are frequent off-target transduction, resulting in antigen presentation by parenchymal cells outside secondary lymphoid organs, and limited cloning capacity for the insertion of multiple or large antigens. For example, the strong tropism of adenoviral vectors for hepatocytes, with >95% of the genetic material being deposited in the liver, leads to generation of functionally impaired $CD8^+$ T cells (24, 25). Major efforts are thus required to engineer adenoviral vectors with improved specificity for the relevant antigen-presenting cells (12, 19). Likewise, lentiviral vectors preferentially infect cells other than DCs, and redirection of their target cell tropism is warranted (26). An additional potential imped-

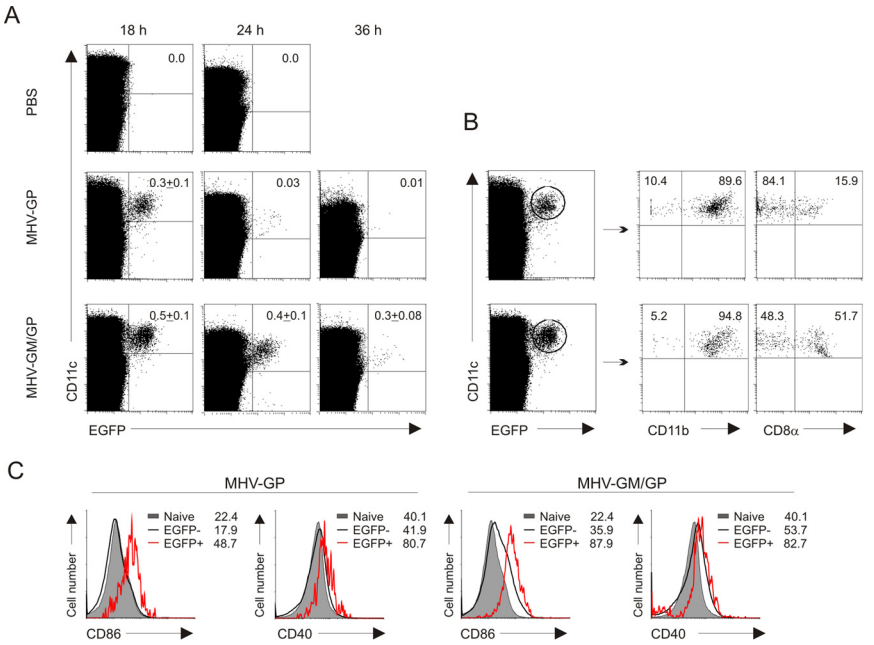

FIG 2 *In vivo* antigen delivery to dendritic cells by MHV-based vaccine vectors. B6 mice were immunized i.v. with 10^6 PFU MHV-GP or MHV-GM/GP or were left untreated. Spleens were collected after 18 h, 24 h, or 36 h and digested with collagenase, and low-density cells were isolated by gradient centrifugation. Expression of CD11c, CD11b, CD8α, CD86, and CD40 on DCs was determined by flow cytometry. (A) Time course analysis of EGFP expression in $CD11c^+$ DCs. Pooled data from two separate experiments (5 mice per time point). Values in the upper right quadrant indicate mean percentages plus SEM of $EGFP^+$ cells. (B) Expression of CD11b and CD8α in transduced DCs at 18 h postinfection. Values in the quadrants represent percentages of $CD11b^+$ or $CD8\alpha^+$ cells in the $EGFP^+$ $CD11c^+$ DCs. (C) DC activation assessed as CD86 and CD40 upregulation on $EGFP^+$ $CD11c^+$ and $EGFP^-$ $CD11c^+$ cells at the 18-h time point. Values in the histograms represent mean fluorescence intensity of the respective population. PBS, phosphate-buffered saline.

iment for the use of DNA-based viral vectors in clinics is their potential to integrate genomic material into the host genome (27).

Coronaviral vectors display a number of features that clearly overcome these limitations. First, replication of these positive-stranded RNA viruses is restricted to the cytoplasm, without a DNA intermediary, making insertion of viral sequences into the host cell genome unlikely. Second, there is accumulating knowledge on how to attenuate coronaviruses in order to provide biosafe vectors (28, 29). Third, coronavirus genomes with sizes of 27 to 31 kb represent the largest autonomously replicating RNAs known to date and thus offer a cloning capacity of more than 6 kb. Fourth, the unique transcription process generates 6 to 8 subgenomic mRNAs encoding the four canonical structural proteins and various numbers of accessory proteins, which can be replaced to encode multiple heterologous proteins (30). Finally, and certainly most intriguing, cell surface receptors of human and murine coronaviruses are expressed on human and murine DCs, respectively (31, 32).

The present study describes the generation and evaluation of rationally designed coronavirus-based vectors that efficiently target antigens and immunostimulatory molecules to DCs. We show that murine-coronavirus-based vectors can deliver multiple antigens and immunostimulatory cytokines almost exclusively to $CD11c^+$ DCs within secondary lymphoid organs. Immunization with only low numbers of particles elicited potent $CD8^+$ T cell responses that provided long-lasting protection against viral challenge. Moreover, single application of these novel viral vectors generated prophylactic and therapeutic immunity against metastatic melanoma. Induction of cytotoxic T lymphocytes (CTL) directed against the human Melan-A (Mel-A) antigen in HLA-A2-transgenic mice and efficient human-DC-mediated stimulation of Mel-A-specific CTL through Mel-A-recombinant human coronavirus 229E (HCoV-229E) indicates that coronavirus-mediated gene transfer to DCs represents a versatile approach for murine and human immunization against both viral infection and cancer.

RESULTS

Design and propagation of biosafe coronavirus-based vaccine vectors. To assess immunogenicity and to ensure maximal safety of coronavirus-based multigene vaccine vectors, we have rationally designed a series of prototype vectors based on the mouse hepatitis virus strain A59 (MHV-A59) (Fig. 1A). With regard to safety, we introduced three basic modifications to obtain replication-competent, but attenuated and propagation-deficient, MHV-based vectors. First, we deleted all MHV accessory genes (*NS2*, *HE*, *gene4*, *gene5a*), a strategy that attenuates MHV in the natural host (29) and provides space for the introduction of heterologous genes. Second, we removed 99 nucleotides within the replicase gene-encoded sequence of nonstructural protein 1 (nsp1), because this deletion has been shown to greatly reduce MHV pathogenicity while retaining immunogenicity (28). Finally, we deleted structural gene *E* to restrict proper particle formation (33). Indeed, although replication of wild-type MHV to maximal titers occurred around day 5 postinfection, *in vivo* replication of MHV vectors could not be detected (not shown). Consequently, there was also no MHV vector replication detectable in livers or brains (not shown). The high safety profile of MHV-based vectors is further illustrated by the fact that the health status of C57BL/6 (B6) or different immunodeficient mice was not affected, even if the vectors were applied at high doses (see Fig. S1 in the supplemental material).

In order to test the coronavirus-based vaccine concept and to develop a vaccine that provides strong CTL responses, in terms of both magnitude and longevity, we used the CTL epitope gp_{33-41} (the region from residues 33 to 41), derived from the lymphocytic choriomeningitis virus (LCMV) glycoprotein, and the Mel-A_{26-35} analog peptide, derived from the human Melan-A/melanoma antigen recognized by T cells 1 (MART1) protein (Fig. 1A). The CTL epitopes were cloned as fusion proteins with the enhanced green fluorescent protein (EGFP) (34, 35), and the corresponding genes, designated *GP-EGFP* and *EGFP–Mel-A*, were cloned between the MHV vector-borne spike and membrane genes. Since appropriate stimulation of DCs is critical for the generation of efficient T cell

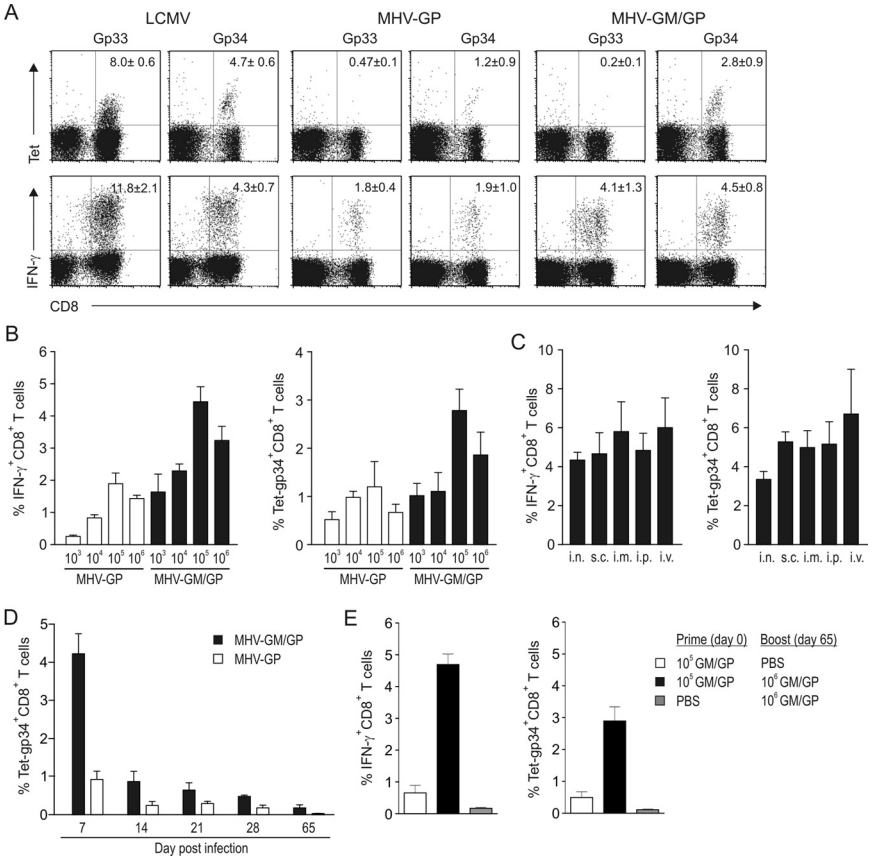

FIG 3 Evaluation of antiviral CD8$^+$ T cell responses. (A) B6 mice were immunized i.v. with either 200 PFU LCMV, 10^5 PFU MHV-GP, or 10^5 PFU MHV-GM/GP. Splenocytes were analyzed on day 7 postinfection (p.i.) for expression of CD8 and reactivity with H2-D^b/gp33 or H2-K^b/gp34 tetramers, and CD8$^+$ splenocytes were analyzed for gp33- and gp34-specific IFN-γ production. Values in the upper right quadrants represent percentages of Tet$^+$ cells ± SEM (upper row) or percentages of IFN-γ^+ cells ± SEM (lower row) in the CD8 T-cell compartment (mean ± SEM; 3 mice per group). (B, C) Efficacy of MHV-based vectors in inducing antiviral CD8$^+$ T cell responses. B6 mice were immunized i.v. with the indicated doses of MHV-GP or MHV-GM/GP. Tetramer analysis and IFN-γ ICS was performed on day 7 postimmunization (mean ± SEM; 3 mice per group). (C) Importance of the route of immunization. B6 mice were immunized with 10^5 PFU MHV-GM/GP. Tetramer analysis and IFN-γ ICS were performed on day 7 postimmunization (mean ± SEM; 2 to 6 mice per group, pooled from 2 different experiments). (D) Duration of vector-induced CD8$^+$ T cell response. B6 mice were immunized with 10^5 PFU MHV-GM/GP or MHV-GP. Tetramer analysis and IFN-γ ICS were performed at the indicated time points (mean ± SEM; 3 mice per group). (E) *In vivo* restimulation of MHV vector-induced CD8$^+$ memory T cells. B6 mice were immunized with 10^5 PFU MHV-GM/GP or injected with PBS. Mice were boosted on day 65 i.v. with 10^6 PFU MHV-GM/GP or injected with PBS. Tetramer analysis and IFN-γ ICS were performed on day 4 after the booster immunization (mean ± SEM; 4 mice per group). i.n., intranasal.

responses (36) and hence an indispensable component of rationally designed vaccines, we inserted the gene encoding the murine granulocyte-macrophage colony-stimulating factor (GM-CSF) between the MHV vector-borne replicase and spike genes (Fig. 1A). To propagate the MHV-based viral vectors to high titers, we produced a packaging cell line based on murine 17clone1 cells that express the MHV envelope (E) protein under the control of the Tet-off system (Fig. 1B). This strategy enabled us to restore efficient vector particle formation and propagation in order to obtain vector stocks of $>10^6$/ml (Fig. 1C).

DC-specific delivery of coronavirus vector-encoded antigens and cytokines. To assess MHV vector growth kinetics on cells that do not express the E protein, we transduced L929 cells, bone marrow-derived CD11c$^+$ DCs, or peritoneal macrophages with the MHV vectors and compared growth kinetics to that of wild-type MHV-A59. In accordance with reports on *E* gene-deficient MHV-A59 (37), the growth of the MHV-based vector was greatly impaired in L929 cells (Fig. 1D). Most importantly, however, MHV vector transduction did not result in particle release in peritoneal macrophages and DCs, demonstrating that the lack of the E protein prevents MHV propagation in primary cells (Fig. 1D). MHV vectors elicited significant EGFP expression in transduced L929 cells and peritoneal macrophages (Fig. 1E) and in CD11c$^+$ DCs (Fig. 1F). Notably, vector-mediated GM-CSF expression resulted in DC activation and maturation, as shown by upregulation of CD86 and CD40 on CD11c$^+$ cells (Fig. 1G). The rapid production of GM-CSF in L929 cells, peritoneal macrophages, and DCs following exposure to the cytokine-encoding vectors (Fig. S2) shows that MHV vectors can be used to simultaneously express antigens and immunostimulatory cytokines in target cells.

To further determine the cellular tropism of MHV-based vectors, we transduced splenocytes from C57BL/6 (B6) mice with MHV-GM/GP *in vitro* and analyzed EGFP expression by flow cytometry. Neither CD4$^+$ nor CD8$^+$ T cells were susceptible to MHV-GM/GP transduction (not shown), whereas antigen-presenting cells, such as B cells (CD19$^+$), macrophages (F4/80$^+$ or CD11b$^+$), and DCs (CD11C$^+$), displayed green fluorescence indicative of MHV vector-mediated EGFP expression (see Fig. S3A in the supplemental material). In order to evaluate whether targeting of DCs and macrophages is also achievable *in vivo*, we injected (intravenously [i.v.]) 10^6 PFU of MHV-GP or MHV-GM/GP into B6 mice and analyzed EGFP expression of splenocytes by flow cytometry. EGFP expression was detectable mainly in CD11c$^+$ CD11b$^+$ DCs and CD11c$^+$ CD8α^+ DCs (Fig. 2A and B and see Fig. S3B in the supplemental material). Finally, we assessed the effects of MHV vector-mediated GM-CSF expression on DC stimulation and activation *in vivo*. Slightly elevated GM-CSF levels in spleens could be observed following application of the MHV-GM/GP vector (Fig. S4A), whereas GM-CSF levels in serum remained below the limit of detection (not shown). Concomitant immunization with MHV-GP and MHV-GM/Mel-A vectors revealed that the supply of GM-CSF in *trans*, i.e., via the MHV-GM/Mel-A vector was not sufficient to achieve the maximal activation of gp34-specific CD8$^+$ T cells. Only when GM-CSF was encoded by the same vector that expressed the GP-EGFP pro-

tein (MHV-GM/GP), was the maximal immune response induced (Fig. S4B). Furthermore, MHV-GM/GP-induced GM-CSF expression did not alter the cellular composition in spleens (see Fig. S5 in the supplemental material). These results support the notion that vector-encoded GM-CSF acts locally in the microenvironment of transduced DCs. However, *in vivo* transduction with both MHV-GP and MHV-GM/GP mediated DC maturation, with upregulation of CD86 and CD40 (Fig. 2C). Notably, application of MHV-GP vectors led to a less efficient transduction of DCs *in vivo*, which lasted only for roughly 18 h (Fig. 2A), suggesting that GM-CSF supplied by MHV vectors fosters DC survival and, to a lesser extent, DC maturation and thereby potentiates their antigen presentation function.

Antiviral CTL responses following coronavirus vector immunization. Infection with LCMV is characterized by a vigorous expansion of antiviral CTL and persistence of protective memory CTL (38), which are directed against several epitopes. Two different epitopes are present in the gp_{33-41} region of the LCMV GP that was used in two of our constructs: the H2-D^b-binding gp_{33-41} (39) and the H2-K^b-binding gp_{34-41} (40). On day 7 after LCMV infection, significant numbers of $CD8^+$ T cells could be detected by MHC tetramer analysis and intracellular cytokine secretion (ICS) assay (Fig. 3A). It is important to note that the gp33 ICS records both gp33- and gp34-specific $CD8^+$ T cells. It appears that the processing of the GP-EGFP transgene in the MHV-GP and MHV-GM/GP vectors permitted the preferential generation of gp34-specific $CD8^+$ T cells to a magnitude comparable to that seen during acute LCMV infection (Fig. 3A). The GM-CSF-encoding MHV vector proved to be highly efficient in the induction of antiviral CTL, even at rather low doses of 10^3 and 10^4 PFU (Fig. 3B). Since the intermediate dose of 10^5 PFU of MHV-GM/GP led to optimal induction of gp34-specific CTL, we used this dose to assess whether application via different routes would influence the induction of transgene-specific CTL. As shown in Fig. 3C, all routes of immunization elicited robust $CD8^+$ T cell responses, with intraperitoneal (i.p.), subcutaneous (s.c.), intramuscular (i.m.), and i.v. injection being the most efficient means of application. Both MHV-GP- and MHV-GM/GP-induced $CD8^+$ T cells displayed full effector function because gp34 peptide-loaded target cells were rapidly eliminated in immunized hosts (see Fig. S6A in the supplemental material). MHV vector-induced $CD8^+$ T cell responses were detectable for more than 65 days after immunization (Fig. 3D) and, most importantly, could be restimulated *in vivo* by immunization with the same vector (Fig. 3E).

Protection against LCMV challenge requires high levels of appropriately activated $CD8^+$ T cells (38). In order to assess the efficacy of MHV vector-based immunization for protection against viral challenge, B6 mice were immunized with graded doses of the MHV-GP or MHV-GM/GP vector and challenged 7 days later with LCMV. Comparable to the high level of $CD8^+$ T cell induction (Fig. 3), complete protection was observed in mice after immunization with a dose of 10^5 PFU (Fig. 4A). Remarkably, as few as 10^3 PFU of MHV-GM/GP still led to a >3-log reduction of LCMV titers in spleens on day 4 postchallenge (Fig. 4A). Protection against LCMV was long-lasting because mice were still protected after more than 2 months following immunization with 10^5 PFU MHV-GM/GP via the i.v. (Fig. 4B), s.c., or i.m. route (see Fig. S6B in the supplemental material). Moreover, the MHV-GM/GP vaccine elicited complete protection against i.p. challenge with LCMV GP recombinant vaccinia virus (VV) (Fig. 4C). Likewise, immunization with MHV-GP provided

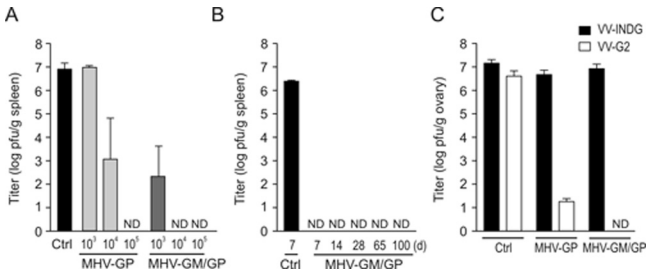

FIG 4 Induction of long-lasting protective antiviral immunity. (A) B6 mice were either left untreated (Ctrl) or immunized (i.v.) with the indicated doses of MHV-GP or MHV-GM/GP. Seven days later, mice were challenged i.v. with 200 PFU LCMV. Viral titers in spleens (means ± SEM) were determined 4 days after LCMV challenge using a focus-forming assay on MC57 cells (4 to 6 mice per group, pooled from 2 different experiments). (B) Duration of protective antiviral immunity. B6 mice were immunized with 10^5 PFU MHV-GM/GP and challenged i.v. with 200 PFU LCMV at the indicated time points. Viral titers in spleens (mean ± SEM) were determined 4 days after LCMV challenge using a focus-forming assay of MC57 cells (4 to 6 mice per group, pooled from 2 different experiments). (C) Female B6 mice were either left untreated (Ctrl) or immunized (i.v.) with 10^5 PFU MHV-GP or 10^5 PFU MHV-GM/GP. Seven days later, mice were challenged i.p. with 2×10^6 PFU LCMV GP-recombinant vaccinia virus (VV-G2) or vesicular stomatitis virus glycoprotein-recombinant vaccinia virus (VV-INDG). Vaccinia virus titers (mean ± SEM) in ovaries were determined 5 days after challenge infection (4 mice per group). ND, not detectable.

substantial protection against this heterologous viral infection (Fig. 4C). It is important to indicate that the MHV-based vaccine, even when GM-CSF was encoded by the vector, provided specific protection because replication of the unrelated recombinant vaccinia virus expressing vesicular stomatitis virus (VSV) Indiana glycoprotein (VV-INDG) was not affected (Fig. 4C). Taken together, these results revealed that the MHV-based vector system is highly efficient in generating protective antiviral immunity and that the incorporation of GM-CSF into the vaccine significantly augmented its protective capacity.

Prophylactic and therapeutic antitumor immunization. In order to evaluate whether MHV vector-based vaccination elicits prophylactic and therapeutic tumor immunity, we resorted to a rapidly growing B16 melanoma model which provides compatibility with the LCMV GP system through expression of a gp33 minigene (B16F10-GP cells) (41). I.v. injection of 5×10^5 B16F10-GP or parental B16F10 cells in control B6 mice resulted in metastatic growth of tumor cells in lungs (Fig. 5A). Immunization with either 10^5 PFU MHV-GP or 10^5 PFU MHV-GM/GP completely blocked the growth of B16F10-GP tumor cells, whereas metastasis formation of the parental B16F10 cells was not affected (Fig. 5A). Application of graded doses of MHV-GP or MHV-GM/GP revealed the high efficacy of this vaccination approach in the prophylactic setting, i.e., 10^4 MHV-GP or only 10^3 PFU MHV-GM/GP were sufficient to prevent the growth of the melanoma cells (Fig. 5B). A long-lasting memory response that provided significant protection against B16F10-GP challenge had been generated following MHV-GM/GP immunization (Fig. 5C). Moreover, the potent $CD8^+$ T cell response elicited through MHV-GM/GP immunization mediated therapeutic tumor immunity (Fig. 5D), i.e., the tumor burden in lungs of B6 mice was significantly reduced even when the vaccine was applied after the tumors had started to form metastatic nodules, indicating that $CD8^+$ T cell re-

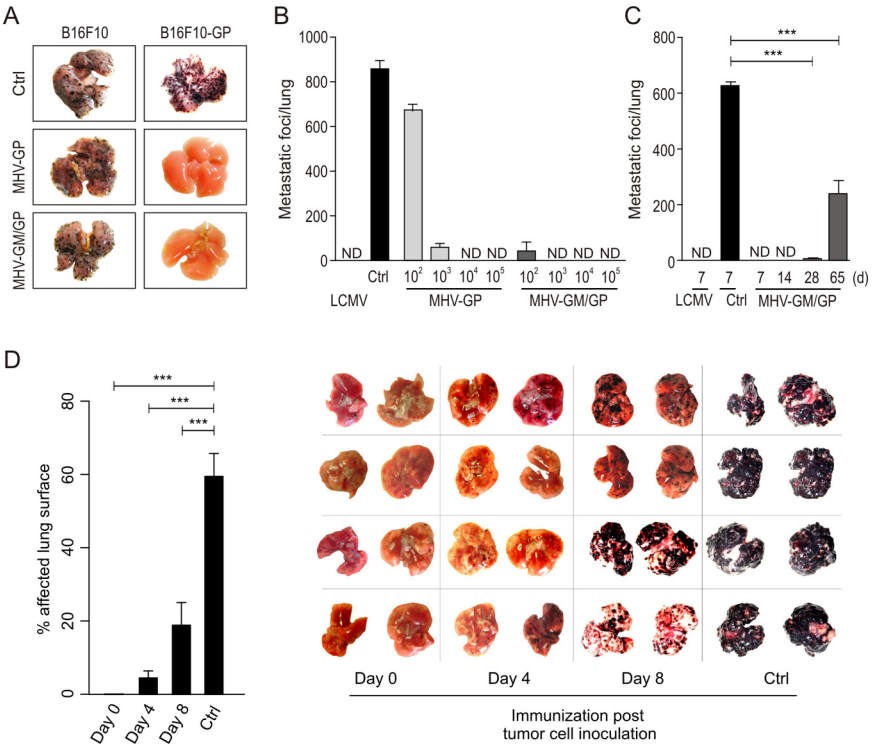

FIG 5 Prevention and immunotherapeutic treatment of metastatic melanoma. (A) B6 mice were either left untreated (Ctrl) or immunized (i.v.) with either 10^5 PFU MHV-GP or MHV-GM/GP. Seven days later, mice were challenged with 5×10^5 LCMV gp33-recombinant B16F10-GP tumor cells or parental B16F10 tumors cells i.v. Tumor growth in lungs was recorded on day 12 after tumor challenge. Macroscopic pictures show representative lungs from 1 out of 3 mice per group. (B) Efficacy of MHV-based vectors in generating prophylactic tumor immunity. B6 mice were immunized i.v. with the indicated doses of MHV-GP or MHV-GM/GP or infected i.v. with 200 PFU LCMV and challenged as described for panel A, and numbers of metastatic foci per lung were determined on day 12 (means ± SEM; 6 mice per group, pooled from 2 experiments). (C) Duration of protective antitumor immunity. B6 mice were immunized i.v. with 10^5 PFU MHV-GM/GP, infected i.v. with 200 PFU LCMV, or left untreated (Ctrl). Mice were challenged as described for panel A, and tumor growth was determined on day (d) 12 postchallenge (means ± SEM; 4 to 6 mice per group, pooled from 2 experiments). (D) Therapeutic antitumor immunity. B6 mice received 5×10^5 LCMV gp33-recombinant B16F10-GP tumor cells i.v. and were immunized with 10^5 PFU MHV-GM/GP i.v. either on the same day (day 0) or 4 or 8 days later. Photographs of dorsal and ventral sides of affected lungs are displayed. Disease severity was determined on day 20 after tumor inoculation; data indicate affected lung surfaces as determined by black pixel counting (mean ± SEM; 4 mice per group). Statistical analysis was performed using Student's *t* test (***, $P < 0.001$; **, $P < 0.01$; *, $P < 0.05$; a P value of >0.05 was not significant). ND, not detectable.

sponses elicited by the novel MHV vectors can exert forceful antitumor activity.

To further substantiate the finding that MHV vectors can induce potent and relevant antitumor $CD8^+$ T cell responses, we employed the human HLA-A2-restricted Melan-A/MART1 system, in which immune responses against the Mel-A_{26-35} analog peptide can be monitored in *HLA-A2.1*-transgenic (A2DR1) mice (42). A2DR1 mice were immunized i.v. with either 10^5 PFU MHV–Mel-A or 10^5 PFU MHV-GM/Mel-A, and Mel-A-specific $CD8^+$ T cell responses were recorded using tetramer analysis and ICS. As shown in Fig. 6A, both vectors elicited substantial $CD8^+$ T cell responses. Time course experiments following i.v. application of MHV-GM/Mel-A revealed a strong global expansion of $CD8^+$ T cells (nearly 10-fold) and a massive expansion of Mel-A-specific $CD8^+$ T cells, with 2×10^6 cells per spleen being tetramer positive and 6×10^6 cells per spleen secreting gamma interferon (IFN-γ) (Fig. 6B). The Mel-A-specific $CD8^+$ T cell population showed a typical contraction after day 7, and a stable memory population had been established by day 28 postimmunization (Fig. 6B). During the acute phase following MHV-GM/GP immunization, >90% of the Mel-A-specific $CD8^+$ T cells had downregulated CD62L (Fig. 6C). As expected, memory $CD8^+$ T cells reacquired CD62L expression, indicating establishment of a central memory $CD8^+$ T cell population. Overall, these results underline that the coronavirus-based vaccination approach, particularly in combination with the immunostimulatory cytokine GM-CSF, provides efficient means for the induction of $CD8^+$ T cell responses against a human tumor antigen.

Delivery of tumor antigen to human DCs. Human coronavirus-based vectors permit specific transfer of multiple genes to DCs because the receptor of HCoV-229E, human aminopeptidase N (hAPN or CD13) (43), is expressed on human DCs (31). Furthermore, we have demonstrated previously that HCoV-229E-based vectors can transduce immature and mature human DCs with reporter genes such as the firefly luciferase gene (30). Here we assessed whether HCoV-229E-mediated delivery of the Mel-A_{26-35} analog peptide to HLA-$A2^+$ human DCs would specifically stimulate human Mel-A-specific $CD8^+$ T cells. To this end, we generated two recombinant human coronaviruses, designated HCoV–Mel-A and HCoV–GP-EGFP, through replacement of HCoV-229E accessory gene 4 with the gene for the EGFP–Mel-A_{26-35} or gp33-EGFP fusion protein, respectively (Fig. 7A). As shown in Fig. 7B, EGFP expression was readily detectable in both human immature and mature DCs after HCoV–Mel-A infection. Time course analysis of human mature DCs infected with HCoV–Mel-A or HCoV–GP-EGFP revealed that high levels of EGFP expression can be reached as early as 9 h postinfection (see Fig. S7 in the supplemental material). Finally, mature DCs infected with HCoV–Mel-A or HCoV–GP-EGFP were employed to stimulate Mel-A_{26-35}-specific human T cells. As shown in Fig. 7C, we observed efficient stimulation of the tumor-specific T cells by HCoV–Mel-A, indicating that HCoV-229E, with its pronounced tropism for human CD13-expressing DCs, represents a particularly promising tool for genetically delivering antigens to human antigen-presenting cells.

DISCUSSION

This study describes a novel vaccine approach that facilitates delivery of viral or tumor antigens to DCs *in vivo*. Concomitant immunostimulation—here via the cytokine GM-CSF—was achieved through targeted transduction by the same viral vector. Single immunization with only 10^4 to 10^5 MHV-based particles

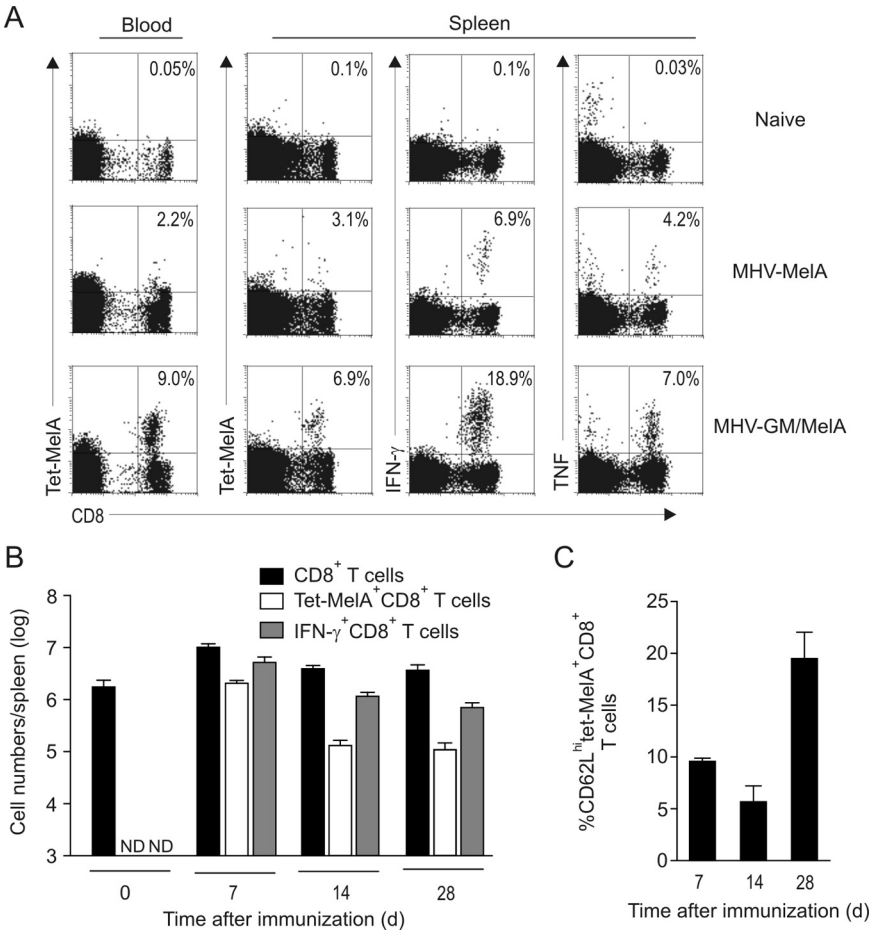

FIG 6 Assessment of anti-Melan-A/MART1 $CD8^+$ T cells in A2DR1 mice. (A) Transgenic mice expressing the human HLA-A2.1 molecule were immunized i.v. with 10^5 PFU MHV–Mel-A or MHV-GM/Mel-A. At day 7 postinfection, splenocytes and mononuclear blood cells were analyzed for expression of CD8 and reactivity with HLA-A2/Mel-A_{26-35} tetramers and for Mel-A_{26-35}-specific IFN-γ and TNF-α production. Values in the upper right quadrants represent mean percentages of Tet^+ cells ± SEM in blood and spleen, percentages of IFN-γ^+ cells ± SEM, or percentages of TNF-α^+ cells ± SEM in the $CD8^+$ T-cell compartment (3 mice per group). (B) Time course of Mel-A_{26-35}-specific $CD8^+$ T-cell responses in A2DR1 mice following i.v. immunization with 10^5 PFU MHV-GM/Mel-A. Total numbers of $CD8^+$ T cells, tetramer-binding Mel-A_{26-35}-specific $CD8^+$ T cells, and Mel-A_{26-35}-specific IFN-γ^+ $CD8^+$ T cells were determined at the indicated time points postimmunization (means ± SEM; 3 mice per group). (C) Differentiation of tetramer-binding Mel-A_{26-35}-specific $CD8^+$ T-cells as determined by CD62L expression at the indicated time points postimmunization (means ± SEM; 3 mice per group). Data are from one representative experiment out of three. hi, high-level expression.

was sufficient to elicit (i) vigorous expansion and optimal differentiation of $CD8^+$ T cells, (ii) protective and long-lasting antiviral immunity, and (iii) prophylactic and therapeutic tumor immunity. Moreover, highly efficient antigen delivery to human DCs with recombinant HCoV-229E and specific stimulation of human $CD8^+$ T cells revealed that this approach is exceptionally well suited for translation into human vaccine studies.

Targeting of antigen to DCs *in vivo* can be achieved by several means (5). The use of viral vectors appears to be the superior strategy for eliciting innate activation of the immune system and optimal induction of $CD8^+$ T cells (24). However, many virus vector systems are still limited in their ability to induce broad and long-lasting immune responses. For example, recombinant adenoviruses have been studied intensively as vaccine candidates mainly because they can be produced to high titers. Nevertheless, high doses of recombinant adenovirus vectors have to be applied to induce an immune response, most probably because they target antigens mainly to nonlymphoid organs, such as the liver (25, 44). In contrast to viral vectors based on DNA viruses (45), positive-stranded RNA virus-based vectors that replicate in the cytoplasm are considered safe vectors. The safety is well documented for vectors based on widely used vaccine strains, such as poliovirus (46), or virus-like particles (VLPs) that contain replicon RNAs devoid of structural genes (47). It should be noted that application of the MHV-based vectors described in this study was always well tolerated and did not result in any sign of disease or adverse side effect irrespectively of dosage and route of MHV-based vector application, even in immunodeficient mouse strains. Finally, it is noteworthy that although some RNA virus-based vectors are able to target DCs (21), their cloning capacity is, in sharp contrast to that of coronavirus-based vectors, generally restricted and the expression of multiple antigens and/or immunostimulatory cytokines is limited.

The novel coronavirus-based vaccine platform described here displayed a high immunogenicity. It is very likely that it is the pronounced tropism of the MHV-based vectors for DCs and macrophages within secondary lymphoid organs that guarantees efficient activation of primary $CD8^+$ T cell responses. *In vivo* imaging studies have shown that $CD169^+$ $CD11c^+$ DCs at the subcapsular sinus of lymph nodes efficiently present viral antigen to naïve T cells (48). Likewise, $CD169^+$ macrophages at the same location are able to collect viral antigen from the lymph and present antigen to follicular B cells (49). Moreover, a recent study from our laboratory has revealed that type I IFN-mediated protection of DCs and macrophages from cytopathic effects of MHV infection is essential to buy time for mounting a protective $CD8^+$ T cell response (50). It remains to be resolved which factors—besides the presence of the MHV receptor on DCs (32)—confers the preferential infection of the relevant antigen-presenting cells within secondary lymphoid organs. For further adaptation of the coronavirus-based vectors to the human system, some of the essential parameters have been clarified; i.e., the receptor of HCoV-229E is expressed mainly on monocytes and DCs within secondary lymphoid organs (31), and recombinant HCoV-229E efficiently targets human DCs irrespective of their maturation status. It is important to add that HCoV-229E is one of at least four human coronaviruses that are transmitted via mucosal surfaces and are associated with mild upper respiratory tract infections (common cold). Furthermore, the low pathogenic potential of

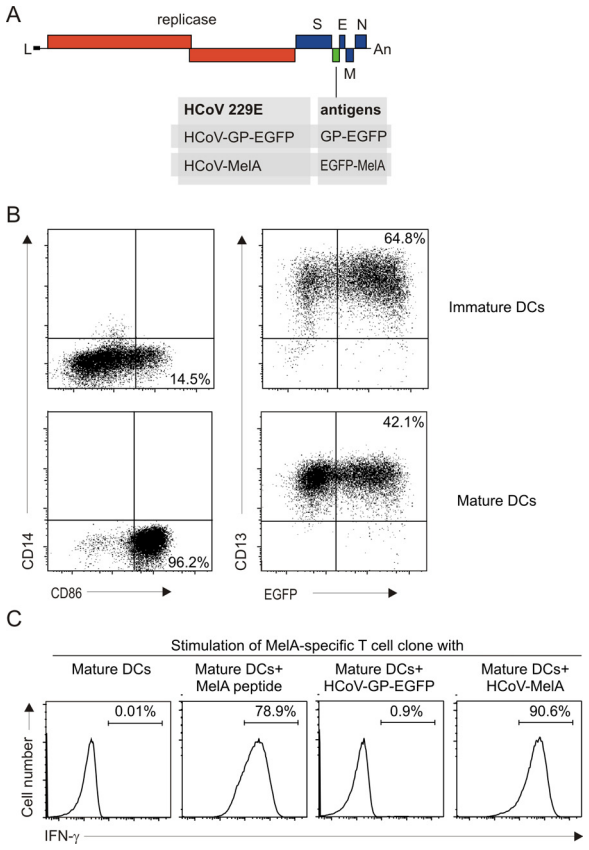

FIG 7 Transduction of human DCs with Melan-A-recombinant HCoV-229E. (A) Schematic representation of the modified HCoV-229E viruses encoding different antigen cassettes. (B) Human monocyte-derived DCs, either immature or mature, were infected with recombinant HCoV-229E (MOI = 1) encoding the EGFP–Mel-A_{26-35} fusion protein. Cells were harvested 12 h later and stained for the indicated surface molecules. (Left) Maturation status as assessed by CD14 and CD86 costaining. Values in the lower right panels indicate percentages of $CD14^-$ $CD86^+$ cells. (Right) Transduction efficacy measured as EGFP expression. Values in the upper right panel indicate percentages of $CD13^+$ $EGFP^+$ cells. The results of one representative experiment out of 4, with DCs derived from different donors, are shown. (C) Activation of a Mel-A-specific T cell clone by Mel-A_{26-35}-presenting DCs. Mature DCs were either left untreated, pulsed with the Mel-A_{26-35} peptide, transduced with GP-EGFP-recombinant HCoV-229E, or transduced with EGFP–Mel-A_{26-35}-recombinant HCoV-229E (MOI = 1). DCs and T cells were cocultured for 6 h at a 4:1 ratio, and activation of the T cells was assessed by IFN-γ ICS. Values in the histogram indicate percentages of IFN-γ-expressing T cells. The results of one representative experiment out of three are shown.

HCoV-229E is corroborated by the fact that HCoV-229E was passaged in volunteers in the 1960s without any serious side effects. These features, together with the pronounced DC-targeting capabilities demonstrated in this report, should encourage the development of coronavirus-based vectors for human use.

A second major advantage of the coronavirus-based vaccination strategy is the large cloning capacity of the vectors, which offers the possibility of incorporating immunostimulatory cytokines. GM-CSF-encoding MHV vectors led to strong production of this cytokine in both macrophages and DCs *in vitro*. Interestingly, GM-CSF expression *in vivo* appeared to be largely restricted to locally transduced cells, as no gross differences in GM-CSF levels in spleen or serum were observed after MHV-GM/GP vector immunization. It is most likely that GM-CSF-induced changes within the microenvironment of transduced macrophages and DCs are decisive for the optimal induction of effector and memory $CD8^+$ T cell responses. Indeed, it is the optimally stimulated expression of costimulatory molecules on antigen-presenting cells, together with sufficient innate immune stimulation, that determines the primary expansion and the maintenance of antiviral $CD8^+$ T cells (51). Accordingly, such non-TCR signals ("signals 2 and 3") are considered key components of rationally designed vaccines (4). The lack of such optimally composed stimuli in a vector-based vaccine most likely requires very elaborate prime-boost immunization regimes, as was recently shown for a combined adenovirus/MVA vaccination approach (52), and/or substantially increased vector doses to achieve efficacy, as for example in vaccination with the latest versions of DC-adapted lentivirus vectors, where application of 5×10^7 to 10×10^7 particles was required to achieve significant expansion of ovalbumin-specific $CD8^+$ T cells in mice (53).

In conclusion, we provide here a versatile vaccine platform based on coronaviruses that achieved the efficient generation of protective immunity, shown as long-lasting memory against viral challenge and induction of both prophylactic and therapeutic tumor immunity. The biology of coronaviruses and the rational modification of these viral RNA vectors harbor significant potential for future development.

MATERIALS AND METHODS

Ethics statement. Experiments were performed in accordance with federal and kantonal guidelines under permission numbers SG07/62, SG07/63, 07/64, and 07/71 following review and approval by the Kantonal Veterinary Office (St. Gallen, Switzerland).

Mice, cells, and viruses. C57BL/6 mice were obtained from Charles River Laboratories (Sulzfeld, Germany). A2DR1 mice were kindly supplied by F. A. Lemonnier (Pasteur Institute, Paris, France) (42). All mice were maintained in individually ventilated cages and were used at between 6 and 9 weeks of age. L929 and CV-1 cells were purchased from the European Collection of Cell Cultures. MC57 and BSC40 cells were obtained from R. M. Zinkernagel (University of Zürich, Switzerland). D980R cells were a kind gift from J. F. Smith (Imperial College London, London, United Kingdom). 17clone1 cells were a kind gift from S. G. Sawicki (Medical University of Ohio, Toledo, OH). Huh7 cells were a kind gift from V. Lohmann (University of Heidelberg, Germany). The LCMV WE strain was obtained from R. M. Zinkernagel (Universität Zürich, Switzerland). Recombinant vaccinia virus expressing LCMV glycoprotein 2 (VV-G2) was originally obtained from B. H. Bishop (University of Oxford, United Kingdom), and recombinant vaccinia virus expressing vesicular stomatitis virus Indiana glycoprotein (VV-INDG) was originally obtained from B. Moss (National Institutes of Health, Bethesda, MD). Titration and determination of antiviral protection assays have been performed as described previously (7). Further details can be found in Text S1 in the supplemental material.

Cloning and generation of recombinant MHV-based vectors and human coronaviruses. Genomic RNA of recombinant MHV-based vectors and recombinant HCoVs were produced from cloned cDNA using purified vaccinia virus DNA as the template for *in vitro* transcription as described previously (54). A detailed description of all cloning steps, sequence information, and production of recombinant coronavirus particles can be found in Text S1 in the supplemental material.

Isolation of dendritic cells and macrophages, flow cytometry, immunofluorescence. Generation of bone marrow-derived DCs and flow cytometric analysis were performed as described previously (50). Further information on these procedures can be found in Text S1 in the supplemental material. For immunofluorescence analysis of viral replication, 2×10^5 L929 cells or peritoneal macrophages were seeded in slide chambers and trans-

duced with MHV-GP or MHV-GM/GP (MOI = 1). At the time points indicated in Fig. 1, the slides were acetone fixed, blocked with the Fc-blocking antibody 2.4G2, and stained with anti-EGFP Alexa 488 (BioLegend). Images were acquired using a Leica DMRA microscope and processed using Adobe Photoshop (Adobe Systems).

Tetramer analysis and intracellular cytokine staining. Peptide-specific $CD8^+$ T cells and *ex vivo* production of IFN-γ or tumor necrosis factor alpha (TNF-α) were determined by tetramer staining, and intracellular cytokine staining was performed as described previously (24, 28). Detailed information on these procedures can be found in Text S1 in the supplemental material.

Melanoma model. B16F10-GP melanoma cells expressing the LCMV gp33 epitope (41) and parental B16F10 cells were kindly provided by H. Pircher (University of Freiburg, Germany). Further information on tumor protection assays can be found in Text S1 in the supplemental material.

Generation of human DCs and ICS. DCs were generated from monocytes isolated from peripheral blood mononuclear cells as described previously (55). Mature DCs were infected with Mel-A/EGFP-recombinant HCoV-229E or GP-EGFP-recombinant HCoV-229E and incubated with Mel-A-specific T cell clones as responder cells. Further details on *in vitro* human $CD8^+$ T cell activation by transduced human DCs can be found in Text S1 in the supplemental material.

Statistical analysis. All statistical analyses were performed with Prism 4.0 (GraphPad Software Inc.). Data were analyzed with the nonpaired Student *t* test under the assumption that the values followed a Gaussian distribution. A P value of <0.05 was considered significant.

ACKNOWLEDGMENTS

We thank Simone Miller, Cornelia Lombardi, and Rita de Giuli for expert technical assistance.

SUPPLEMENTAL MATERIAL

Supplemental material for this article may be found at http://mbio.asm.org/lookup/suppl/doi:10.1128/mBio.00171-10/-/DCSupplemental.

Text S1, DOC file, 0.113 MB.
FIG S1, TIF file, 1.956 MB.
FIG S2, TIF file, 2.980 MB.
FIG S3, TIF file, 1.303 MB.
FIG S4, TIF file, 1.249 MB.
FIG S5, TIF file, 2.474 MB.
FIG S6, TIF file, 2.450 MB.
FIG S7, TIF file, 2.685 MB.

REFERENCES

1. **McMichael, A. J.** 2006. HIV vaccines. Annu. Rev. Immunol. **24**:227–255.
2. **Strickland, G. T., S. S. El Kamary, P. Klenerman, and A. Nicosia.** 2008. Hepatitis C vaccine: supply and demand. Lancet Infect. Dis. **8**:379–386.
3. **Melief, C. J.** 2008. Cancer immunotherapy by dendritic cells. Immunity **29**:372–383.
4. **Appay, V., D. C. Douek, and D. A. Price.** 2008. CD8+ T cell efficacy in vaccination and disease. Nat. Med. **14**:623–628.
5. **Tacken, P. J., I. J. de Vries, R. Torensma, and C. G. Figdor.** 2007. Dendritic-cell immunotherapy: from ex vivo loading to in vivo targeting. Nat. Rev. Immunol. **7**:790–802.
6. **Steinman, R. M., and J. Banchereau.** 2007. Taking dendritic cells into medicine. Nature **449**:419–426.
7. **Ludewig, B., S. Ehl, U. Karrer, B. Odermatt, H. Hengartner, and R. M. Zinkernagel.** 1998. Dendritic cells efficiently induce protective antiviral immunity. J. Virol. **72**:3812–3818.
8. **Ludewig, B., K. J. Maloy, C. Lopez-Macias, B. Odermatt, H. Hengartner, and R. M. Zinkernagel.** 2000. Induction of optimal anti-viral neutralizing B cell responses by dendritic cells requires transport and release of virus particles in secondary lymphoid organs. Eur. J. Immunol. **30**:185–196.
9. **Ludewig, B., S. Oehen, F. Barchiesi, R. A. Schwendener, H. Hengartner, and R. M. Zinkernagel.** 1999. Protective antiviral cytotoxic T cell memory is most efficiently maintained by restimulation via dendritic cells. J. Immunol. **163**:1839–1844.
10. **Ludewig, B., A. F. Ochsenbein, B. Odermatt, D. Paulin, H. Hengartner, and R. M. Zinkernagel.** 2000. Immunotherapy with dendritic cells directed against tumor antigens shared with normal host cells results in severe autoimmune disease. J. Exp. Med. **191**:795–804.
11. **Specht, J. M., G. Wang, M. T. Do, J. S. Lam, R. E. Royal, M. E. Reeves, S. A. Rosenberg, and P. Hwu.** 1997. Dendritic cells retrovirally transduced with a model antigen gene are therapeutically effective against established pulmonary metastases. J. Exp. Med. **186**:1213–1221.
12. **Rea, D., M. J. Havenga, M. van Den Assem, R. P. Sutmuller, A. Lemckert, R. C. Hoeben, A. Bout, C. J. Melief, and R. Offringa.** 2001. Highly efficient transduction of human monocyte-derived dendritic cells with subgroup B fiber-modified adenovirus vectors enhances transgene-encoded antigen presentation to cytotoxic T cells. J. Immunol. **166**:5236–5244.
13. **Palucka, A. K., H. Ueno, J. W. Fay, and J. Banchereau.** 2007. Taming cancer by inducing immunity via dendritic cells. Immunol. Rev. **220**:129–150.
14. **Bonifaz, L. C., D. P. Bonnyay, A. Charalambous, D. I. Darguste, S. Fujii, H. Soares, M. K. Brimnes, B. Moltedo, T. M. Moran, and R. M. Steinman.** 2004. In vivo targeting of antigens to maturing dendritic cells via the DEC-205 receptor improves T cell vaccination. J. Exp. Med. **199**:815–824.
15. **Tacken, P. J., I. J. de Vries, K. Gijzen, B. Joosten, D. Wu, R. P. Rother, S. J. Faas, C. J. Punt, R. Torensma, G. J. Adema, and C. G. Figdor.** 2005. Effective induction of naive and recall T-cell responses by targeting antigen to human dendritic cells via a humanized anti-DC-SIGN antibody. Blood **106**:1278–1285.
16. **Meyer-Wentrup, F., D. Benitez-Ribas, P. J. Tacken, C. J. Punt, C. G. Figdor, I. J. de Vries, and G. J. Adema.** 2008. Targeting DCIR on human plasmacytoid dendritic cells results in antigen presentation and inhibits IFN-alpha production. Blood **111**:4245–4253.
17. **Steinman, R. M.** 2008. Dendritic cells in vivo: a key target for a new vaccine science. Immunity **29**:319–324.
18. **Rea, D., M. E. Johnson, M. J. Havenga, C. J. Melief, and R. Offringa.** 2001. Strategies for improved antigen delivery into dendritic cells. Trends Mol. Med. **7**:91–94.
19. **Cheng, C., J. G. Gall, W. P. Kong, R. L. Sheets, P. L. Gomez, C. R. King, and G. J. Nabel.** 2007. Mechanism of AD5 vaccine immunity and toxicity: fiber shaft targeting of dendritic cells. PLoS Pathog. **3**:e25.
20. **Ageichik, A., M. K. Collins, and M. Dewannieux.** 2008. Lentivector targeting to dendritic cells. Mol. Ther. **16**:1008–1009.
21. **Flatz, L., A. N. Hegazy, A. Bergthaler, A. Verschoor, C. Claus, M. Fernandez, L. Gattinoni, S. Johnson, F. Kreppel, S. Kochanek, M. Broek, A. Radbruch, F. Levy, P. H. Lambert, C. A. Siegrist, N. P. Restifo, M. Lohning, A. F. Ochsenbein, G. J. Nabel, and D. D. Pinschewer.** 2010. Development of replication-defective lymphocytic choriomeningitis virus vectors for the induction of potent CD8+ T cell immunity. Nat. Med. **16**:339–345.
22. **Nishimoto, K. P., A. K. Laust, K. Wang, K. I. Kamrud, B. Hubby, J. F. Smith, and E. L. Nelson.** 2007. Restricted and selective tropism of a Venezuelan equine encephalitis virus-derived replicon vector for human dendritic cells. Viral Immunol. **20**:88–104.
23. **Polo, J. M., J. P. Gardner, Y. Ji, B. A. Belli, D. A. Driver, S. Sherrill, S. Perri, M. A. Liu, and T. W. Dubensky, Jr..** 2000. Alphavirus DNA and particle replicons for vaccines and gene therapy. Dev. Biol. (Basel) **104**:181–185.
24. **Krebs, P., E. Scandella, B. Odermatt, and B. Ludewig.** 2005. Rapid functional exhaustion and deletion of CTL following immunization with recombinant adenovirus. J. Immunol. **174**:4559–4566.
25. **Yang, T. C., J. Millar, T. Groves, N. Grinshtein, R. Parsons, S. Takenaka, Y. Wan, and J. L. Bramson.** 2006. The CD8+ T cell population elicited by recombinant adenovirus displays a novel partially exhausted phenotype associated with prolonged antigen presentation that nonetheless provides long-term immunity. J. Immunol. **176**:200–210.
26. **Lopes, L., M. Dewannieux, U. Gileadi, R. Bailey, Y. Ikeda, C. Whittaker, M. P. Collin, V. Cerundolo, M. Tomihari, K. Ariizumi, and M. K. Collins.** 2008. Immunization with a lentivector that targets tumor antigen expression to dendritic cells induces potent CD8+ and CD4+ T-cell responses. J. Virol. **82**:86–95.
27. **Dobbelstein, M.** 2003. Viruses in therapy—royal road or dead end? Virus Res. **92**:219–221.
28. **Züst, R., L. Cervantes-Barragan, T. Kuri, G. Blakqori, F. Weber, B. Ludewig, and V. Thiel.** 2007. Identification of coronavirus non-structural protein 1 as a major pathogenicity factor—implications for the rational design of live attenuated coronavirus vaccines. PLoS Pathog. **3**:e109.
29. **de Haan, C. A., P. S. Masters, X. Shen, S. Weiss, and P. J. Rottier.** 2002. The group-specific murine coronavirus genes are not essential, but their

deletion, by reverse genetics, is attenuating in the natural host. Virology **296**:177–189.
30. **Thiel, V., N. Karl, B. Schelle, P. Disterer, I. Klagge, and S. G. Siddell.** 2003. Multigene RNA vector based on coronavirus transcription. J. Virol. **77**:9790–9798.
31. **Summers, K. L., B. D. Hock, J. L. McKenzie, and D. N. Hart.** 2001. Phenotypic characterization of five dendritic cell subsets in human tonsils. Am. J. Pathol. **159**:285–295.
32. **Zhou, H., and S. Perlman.** 2006. Preferential infection of mature dendritic cells by mouse hepatitis virus strain JHM. J. Virol. **80**:2506–2514.
33. **Ortego, J., D. Escors, H. Laude, and L. Enjuanes.** 2002. Generation of a replication-competent, propagation-deficient virus vector based on the transmissible gastroenteritis coronavirus genome. J. Virol. **76**: 11518–11529.
34. **Oehen, S., T. Junt, C. Lopez-Macias, and T. A. Kramps.** 2000. Antiviral protection after DNA vaccination is short lived and not enhanced by CpG DNA. Immunology **99**:163–169.
35. **Valmori, D., F. Levy, I. Miconnet, P. Zajac, G. C. Spagnoli, D. Rimoldi, D. Lienard, V. Cerundolo, J. C. Cerottini, and P. Romero.** 2000. Induction of potent antitumor CTL responses by recombinant vaccinia encoding a melan-A peptide analogue. J. Immunol. **164**:1125–1131.
36. **Steinman, R. M., D. Hawiger, and M. C. Nussenzweig.** 2003. Tolerogenic dendritic cells. Annu. Rev. Immunol. **21**:685–711.
37. **Kuo, L., and P. S. Masters.** 2003. The small envelope protein E is not essential for murine coronavirus replication. J. Virol. **77**:4597–4608.
38. **Wherry, E. J., and R. Ahmed.** 2004. Memory CD8 T-cell differentiation during viral infection. J. Virol. **78**:5535–5545.
39. **Pircher, H., D. Moskophidis, U. Rohrer, K. Burki, H. Hengartner, and R. M. Zinkernagel.** 1990. Viral escape by selection of cytotoxic T cell-resistant virus variants in vivo. Nature **346**:629–633.
40. **Hudrisier, D., M. B. Oldstone, and J. E. Gairin.** 1997. The signal sequence of lymphocytic choriomeningitis virus contains an immunodominant cytotoxic T cell epitope that is restricted by both H-2D(b) and H-2K(b) molecules. Virology **234**:62–73.
41. **Prevost-Blondel, A., C. Zimmermann, C. Stemmer, P. Kulmburg, F. M. Rosenthal, and H. Pircher.** 1998. Tumor-infiltrating lymphocytes exhibiting high ex vivo cytolytic activity fail to prevent murine melanoma tumor growth in vivo. J. Immunol. **161**:2187–2194.
42. **Pajot, A., M. L. Michel, N. Fazilleau, V. Pancre, C. Auriault, D. M. Ojcius, F. A. Lemonnier, and Y. C. Lone.** 2004. A mouse model of human adaptive immune functions: HLA-A2.1-/HLA-DR1-transgenic H-2 class I-/class II-knockout mice. Eur. J. Immunol. **34**:3060–3069.
43. **Yeager, C. L., R. A. Ashmun, R. K. Williams, C. B. Cardellichio, L. H. Shapiro, A. T. Look, and K. V. Holmes.** 1992. Human aminopeptidase N is a receptor for human coronavirus 229E. Nature **357**:420–422.
44. **Engelhardt, J. F., X. Ye, B. Doranz, and J. M. Wilson.** 1994. Ablation of E2A in recombinant adenoviruses improves transgene persistence and decreases inflammatory response in mouse liver. Proc. Natl. Acad. Sci. U. S. A. **91**:6196–6200.
45. **Trono, D.** 2003. Virology. Picking the right spot. Science **300**:1670–1671.
46. **Crotty, S., B. L. Lohman, F. X. Lu, S. Tang, C. J. Miller, and R. Andino.** 1999. Mucosal immunization of cynomolgus macaques with two serotypes of live poliovirus vectors expressing simian immunodeficiency virus antigens: stimulation of humoral, mucosal, and cellular immunity. J. Virol. **73**:9485–9495.
47. **Harvey, T. J., I. Anraku, R. Linedale, D. Harrich, J. Mackenzie, A. Suhrbier, and A. A. Khromykh.** 2003. Kunjin virus replicon vectors for human immunodeficiency virus vaccine development. J. Virol. **77**: 7796–7803.
48. **Hickman, H. D., K. Takeda, C. N. Skon, F. R. Murray, S. E. Hensley, J. Loomis, G. N. Barber, J. R. Bennink, and J. W. Yewdell.** 2008. Direct priming of antiviral CD8+ T cells in the peripheral interfollicular region of lymph nodes. Nat. Immunol. **9**:155–165.
49. **Junt, T., E. A. Moseman, M. Iannacone, S. Massberg, P. A. Lang, M. Boes, K. Fink, S. E. Henrickson, D. M. Shayakhmetov, N. C. Di Paolo, N. van Rooijen, T. R. Mempel, S. P. Whelan, and U. H. von Andrian.** 2007. Subcapsular sinus macrophages in lymph nodes clear lymph-borne viruses and present them to antiviral B cells. Nature **450**:110–114.
50. **Cervantes-Barragan, L., U. Kalinke, R. Zust, M. Konig, B. Reizis, C. Lopez-Macias, V. Thiel, and B. Ludewig.** 2009. Type I IFN-mediated protection of macrophages and dendritic cells secures control of murine coronavirus infection. J. Immunol. **182**:1099–1106.
51. **Harty, J. T., and V. P. Badovinac.** 2008. Shaping and reshaping CD8+ T-cell memory. Nat. Rev. Immunol. **8**:107–119.
52. **Draper, S. J., A. C. Moore, A. L. Goodman, C. A. Long, A. A. Holder, S. C. Gilbert, F. Hill, and A. V. Hill.** 2008. Effective induction of high-titer antibodies by viral vector vaccines. Nat. Med. **14**:819–821.
53. **Yang, L., H. Yang, K. Rideout, T. Cho, K. I. Joo, L. Ziegler, A. Elliot, A. Walls, D. Yu, D. Baltimore, and P. Wang.** 2008. Engineered lentivector targeting of dendritic cells for in vivo immunization. Nat. Biotechnol. **26**:326–334.
54. **Eriksson, K. K., D. Makia, and V. Thiel.** 2008. Generation of recombinant coronaviruses using vaccinia virus as the cloning vector and stable cell lines containing coronaviral replicon RNAs. Methods Mol. Biol. **454**: 237–254.
55. **Waeckerle-Men, Y., E. U. Allmen, R. von Moos, B. J. Classon, E. Scandella, H. P. Schmid, B. Ludewig, M. Groettrup, and S. Gillessen.** 2005. Dendritic cells generated from patients with androgen-independent prostate cancer are not impaired in migration and T-cell stimulation. Prostate **64**:323–331.